Supplementary Information

Supplemental Methods

Flow cytometry. All flow cytometry analysis was done using a Beckman Coulter Cyan ADP flow cytometer using Summitv4.1 software (Dakocytomation). GFP expression was measured after fixation of cells in 4% PFA for 20 minutes at room temperature. Total cellular F-actin content was measured by Alexa647-Phalloidin (Invitrogen) staining of PFA fixed and Perm/Wash (BD Biosceinces) permeabilised cells as previously described[5]. Apoptosis was measured by staining unfixed cells with AnnexinV-Cy5 (Autogen Bioclear UK) and propidium iodide. DNA synthesis was assayed by measuring EdU incorporation using the Click-iT EdU cell proliferation assay (Invitrogen).

Cytospins and cell morphology. Cytospins were prepared using a Shandon II cytocentrifuge. After air drying, cells were stained with Diff -Quick (Medion Diagnostics) and analyzed under a 40x objective. 10 random fields (totalling ~1,000 cells) were counted from each slide. Micronuclei were defined as a nuclear body less than 30% the size of the main nuclei. HT1080 cells were stained in 12 well plates.

Western Blotting

Protein lysates were separated on 4 – 12% NuPage gels (Invitrogen) transferred to PVDF membranes and probed with antibodies using standard techniques. Antibodies used were Aurora B (Abcam ab2254), GFP (Santa Cruz sc8334), β-actin and β-tubulin (Sigma Aldrich clones AC-15 and Tub2.1). Horseradish peroxidase – conjugated secondary antibody (GE Healthcare) was detected using supersignal west pico substrate (Pierce Chemical Co.) and an Uvichemi documentation system (Uvitech).

Timelapse wide-field microscopy. Cells were transduced 3-7 days prior to imaging. Cells were seeded in 12 well plates cultured in a humidified 5% CO_2 atmosphere at 37^{o}C on a temperature controlled Zeiss Axiovert 135 microscope. Multipoint imaging was used so that control and experimental cultures were imaged side by side to avoid any variation between measurement conditions. Images were captured every 60 seconds through a 32x's objective (NA 0.4) with a Hamamatsu ORCA-ER CCD camera. The whole system was run using Volocity software (Perkin Elmer). Image analysis was done with both Volocity software and Image J (NIH). Key stages of mitosis were marked manually to determine mitotic timings. NEB was defined as the point when the nuclear envelope was no longer present in phase contrast images, and coincided with the first signs of chromosome condensation. Anaphase was timed from the first sign of chromatid separation. Furrow ingression was timed from the first frame where an indent was visible in both edges of the cell. Furrow was considered complete when the furrow diameter was less than 4 μm. Measurement of distance between separating bodies of chromatids in anaphase was achieved by manual marking using ImageJ software. The measurements were from the centre mass of the separating chromatids, marked on both phase contrast and red fluorescence (H2B-cherry) channels. Speeds were calculated from the distance between the bodies of chromatids measured every 60 seconds. Speed was defined as distance (nm) divided by 2 divided by 60 seconds. The speeds are therefore the speed that chromatids move away from the centre of the cell. Furrow diameter was measured manually in ImageJ from phase contrast images. Speed was defined as distance from one edge of the furrow to the other (nm) divided by 2 divided by 60 seconds. The speed of furrow closure is therefore the speed that an edge of the furrow moves towards the centre of the cell. The measurements presented start at the last frame where the cell was round, so encompass the entire contraction of the cell across the plane of division.

Atomic Force Microscopy. All measurements were effected with a JPK Nanowizard (JPK, Berlin, Germany) using MSNL cantilevers with a nominal spring constant of k=0.01 N/m (Veeco,

UK). Cantilevers were calibrated using the thermal noise method implemented in the JPK software. After calibration, the AFM cantilevers were modified with a latex microsphere (Fluorospheres, Invitrogen, Paisley, UK) to simplify the tip geometry. Elasticity was measured by fitting the approach part of force-distance curves with the Hertz model for spherical contact. Viscosity was measured by rapidly applying a force onto the cell with an AFM cantilever and monitoring force relaxation over time at several locations on each cell. Force-relaxation curves were analysed by assuming that the cell behaved as a viscoelastic solid and fit with[1]:

$F(t) = \frac{4}{3}\frac{R^{0.5}\delta_0^{3/2}}{1-\nu}\left(k_1 + k_2 e^{-\frac{k_2 t}{\mu}}\right)$. where R is the radius of the indenter, $\nu = 0.5$ the Poisson ratio, μ is the apparent viscosity and k_1 and k_2 have units of elasticities with the cellular elasticity $E = \frac{2}{3}k_1$.

Multiple measurements were made on different areas of each cell examined (n>27 control, CA-WASp, CA-WASp + 40 μM CK666, n>161 individual measurements, and for CA-WASp + 20 μM CK666 n=6 cells with n=35 individual measurements).

Spinning disk timelapse confocal microscopy. HT1080 cells stably expressing lifeact-ruby, or GFP-CenpA where grown on glass bottom dishes and imaged on either an UltraView Vox (Perkin Elmer) spinning disc system was used with 60x oil immersion objective (NA 1.4) or Olympus IX81 Andor system with 100x oil immersion objective (NA 1.4) fitted with a 37°C environmental chamber. 7 z-sections at 2 μm separation were taken at 1 minute intervals for Life-act-ruby imaging in cells expressing GFP-WASp fusion proteins. For kinetochore oscillations we took 20 z-sections at 0.5 μm separation were taken at 7.5 second intervals over 5 minutes as described [2]. Acquisition was optimised for minimum laser power such that mitotic timings were not perturbed by imaging.

Confocal Microscopy. HT1080 cells were grown on glass coverslips. U937 cells were attached to poly-L-Lysine (Sigma-Aldrich) coated glass coverslips for 30 minutes. For analysis of F-actin density, lagging chromosomes and GFP-WASp expression cells were fixed in 4% PFA for 20 minutes at room temperature, and rinsed in PBS. Permeabilisation was achieved with 0.2% TX-100 for 3 minutes. F-actin was stained with Alexa647-Phalloidin (Invitrogen) for 20 minutes and nuclei were stained with 1uM DAPI for 5 minutes. Coverslips were mounted using prolong gold antifade reagent (Invitrogen) and analyzed using a Zeiss LSM 710 inverted confocal microscope with a 40x C-Apochromat NA 1.2 WD 280 mm objective. Imaging used the optimal pixel width (maximum 0.13 μm) and optical sections were taken at the optimal separation (0.38 – 0.44 μm). Image analysis used ImageJ software (NIH). F-actin density was estimated by measuring the intensity of phalloidin staining in a circle with an area of approximately 40 μm^2 over at least 2 optical sections in at least 3 locations in the cytoplasm of HT1080 cells, or around prometaphase chromosomes in HT1080 and U937 cells. The average intensity from each reading was taken, so the readings around prometaphase chromosomes underestimate the true increase in F-actin as it includes the regions with no F-actin where chromosomes are located.

Cold stable metaphase arrested microtubule staining was performed on cells treated with 5 μM MG132 for 3 hours to accumulate cells at the end of metaphase, followed by 10 minutes incubation in ice cold media[3]. Cells were fixed in -20^{o}C methanol for 2 minutes, then permeabilised in 0.2% TX-100 for 3 minutes. Antibodies were diluted in TBS/ 0.1% tween with 1% BSA and 5% goat serum and incubated on cells sequentially after blocking for 1 hour. Antibodies used were Rat anti-α-tubulin (Sigma), Mouse anti-Hec1 (Abcam), and Alexa 647 and Alexa 568 conjugated secondary antibodies (Invitrogen). Images were taken with a 63x Plan-Apochromat NA 1.4 oil immersion objective. Pixel sizes were 50 nm x-y and 350 nm z. Total kMT intensity was calculated from the sum of α-tubulin immunofluorescence in the spindle from all z sections through the entire cell. Individual kMT bundles were measured from the α-tubulin immunofluorescence of single z-sections of the kMT bundle adjacent to the kinetochore

(as defined by Hec1 staining) over an area of 0.5 x 0.5 μm. All images in each repeat of the experiment were collected on the same day using identical acquisition settings, and were normalised to the mean control value from each experiment.

Supplemental References

1. Darling EM, Zauscher S, Guilak F. Viscoelastic properties of zonal articular chondrocytes measured by atomic force microscopy. *Osteoarthritis Cartilage*. 2006;14(6):571-579.
2. Jaqaman K, King EM, Amaro AC, et al. Kinetochore alignment within the metaphase plate is regulated by centromere stiffness and microtubule depolymerases. *J Cell Biol*. 2010;188(5):665-679.
3. Maldonado M, Kapoor TM. Constitutive Mad1 targeting to kinetochores uncouples checkpoint signalling from chromosome biorientation. *Nature cell biology*. 2011;13(4):475-482.

Figure S1 Timing of key stages of cell division in Control and CA-WASp HT1080 cells

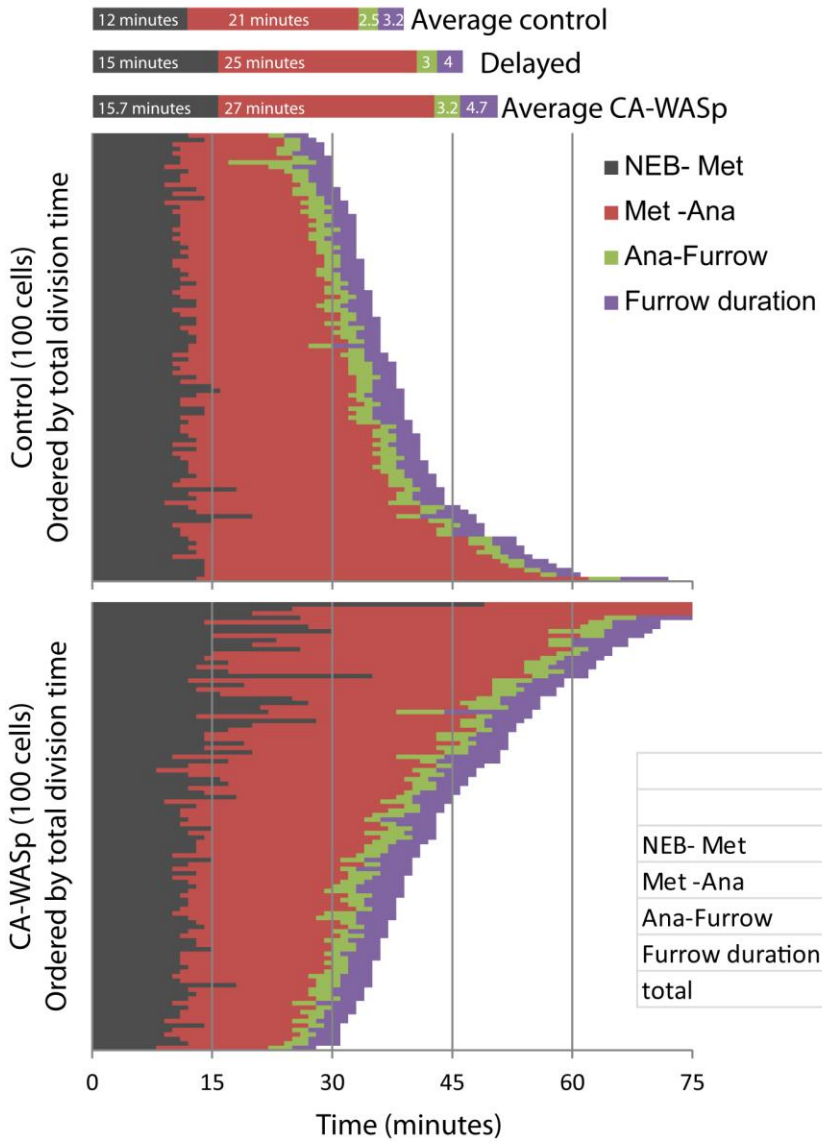

	Time in minutes		
	Control	CA-WASp	t-test
NEB- Met	11.8 ± 1.8	15.7 ± 6.5	< 0.0001
Met -Ana	21.4 ± 7.7	27.0 ± 11.7	0.0082
Ana-Furrow	2.6 ± 1.0	3.2 ± 1.1	< 0.0001
Furrow duration	3.2 ± 0.9	4.7 ± 1.5	< 0.0001
total	38.9 ± 8.3	50.6 ± 16.5	< 0.0001

Figure S1. Timing of mitotic events in Control and CA-WASp HT1080 cells. 100 cells were assessed for each treatment, and timings recorded for NEB, metaphase alignment/ congression, anaphase, furrow initiation and furrow completion. Each horizontal bar on the graph represents one cell. The mean duration of a typical control division is shown above the graph, followed by our definition of a delayed division, and the mean duration of mitosis in a cell expressing CA-WASp. The table shows the mean times and standard deviations for each stage of mitosis, and the p-value from a two-tailed students t-test.

Figure S2 F-actin rapidly accumulates in the nucleus following NEB, and is removed by Arp2/3 inhibition

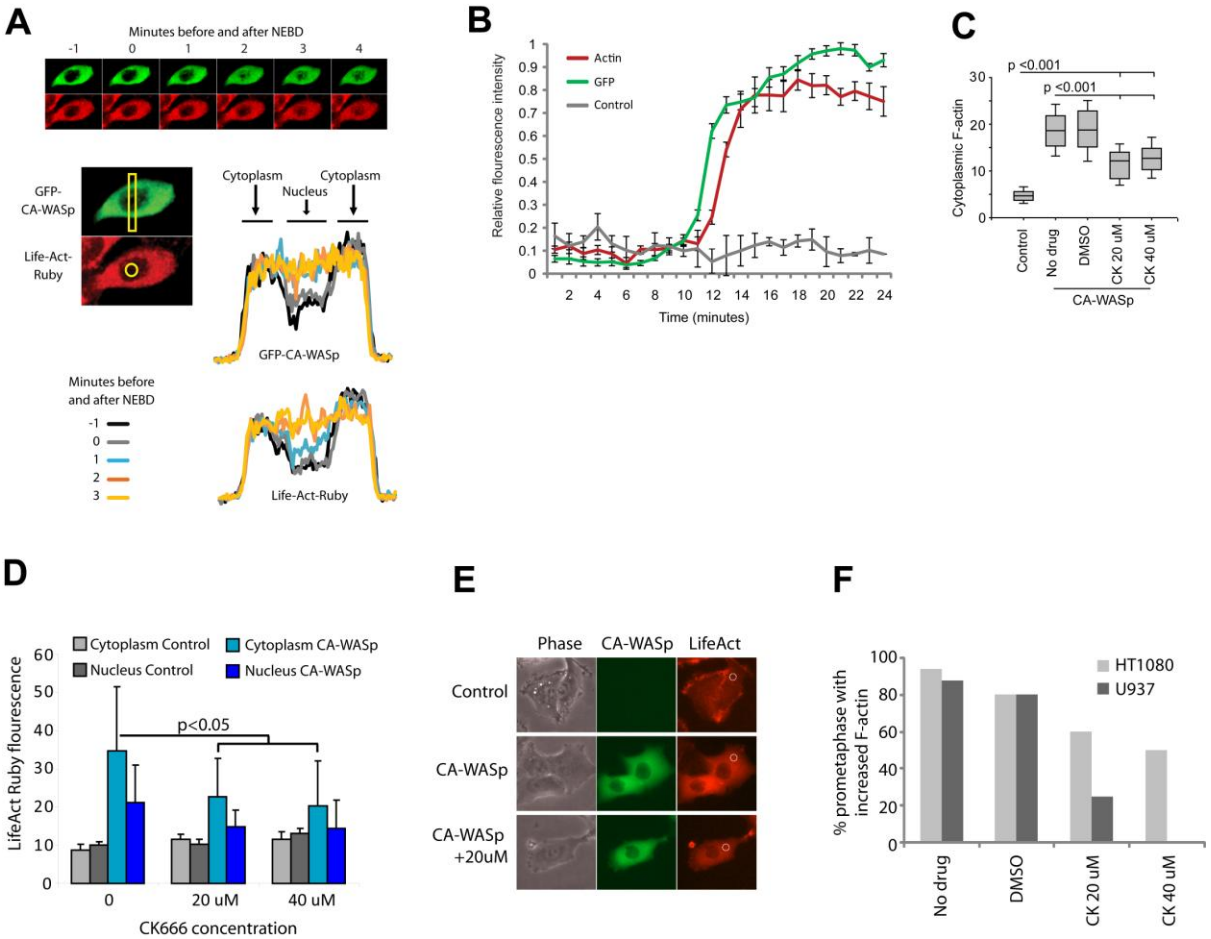

Figure S2. F-actin rapidly accumulates in the nucleus following NEB, and is removed by Arp2/3 inhibition (**A**) Spinning disk live cell imaging of HT1080 cell NEB showing entry of GFP-CA-WASp to the nucleus followed by Life-Act binding to F-actin. GFP-CA-WASp and Life-Act intensity were measured in cross sections (**A**) and areas within the nucleus (**B**) showing a rapid rise in Life-Act within the nucleus in CA-WASp cells, but not in controls. (**C**) Cytoplasmic F-actin levels (arbitrary units) in HT1080 controls and cells expressing CA-WASp cultured in the conditions shown. n > 10 for each condition. (**D, E**) Nuclear and cytoplasmic LifeAct-Ruby and GFP-CA-WASp was measured in HT1080 cells treated with CK666. (**F**) Comparison of the percent of HT1080 and U937 cells expressing CA-WASp that showed an abnormal increase in nuclear F-actin at prometaphase. The inhibition of Arp2/3 complex is more successful at preventing this abnormal F-actin accumulation in the U937 than the HT1080 cell line.

Figure S3 Arp2/3 complex inhibition rescues the proliferative defects caused by CA-WASp.

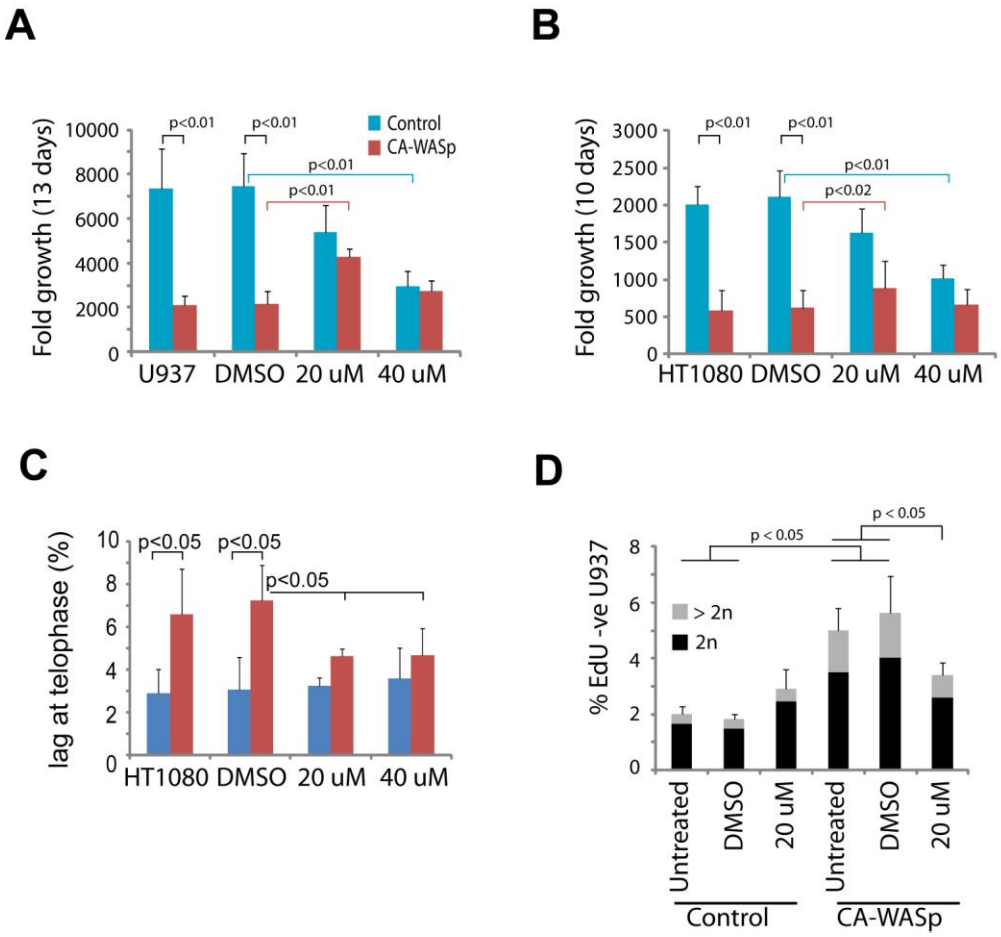

Figure S3. Arp2/3 complex inhibition rescues the proliferative defects caused by CA-WASp. (**A, B**) Fold growth of (**A**) U937 cells over 13 days and (**B**) HT1080 cells over 10 days. (**C**) Percent of HT1080 cells with lagging chromosomes telophase, n = 3 with at least 300 cells analyzed per condition. (**D**) Percent of U937 cells that fail to enter S-phase (incorporate any BrdU analog EdU) during 22 hours of culture measured by flow cytometry, n = 5.

Figure S4 Kinetic events during mitosis are slower in cells expressing CA-WASp.

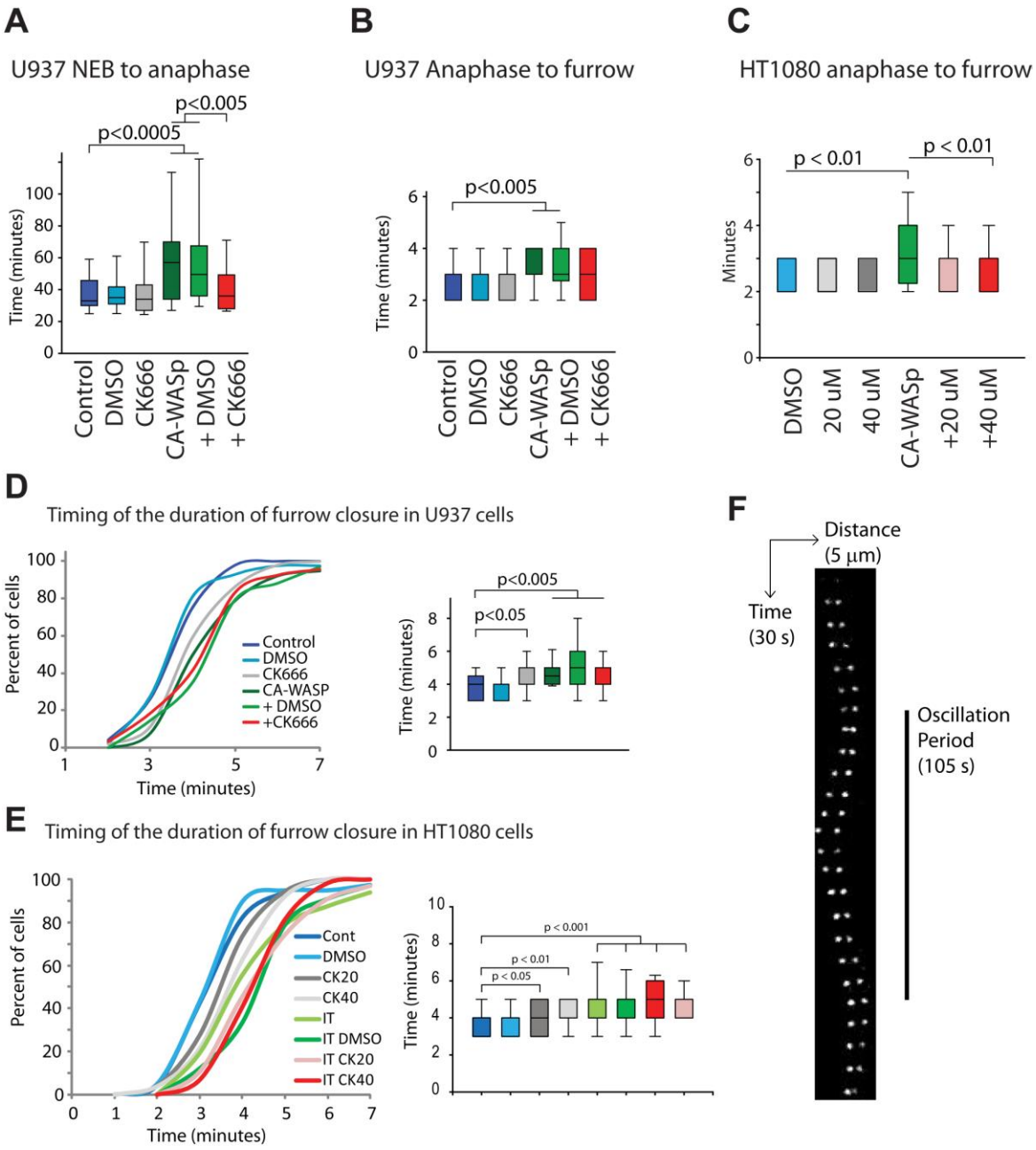

Figure S4. Kinetic events during mitosis are slower in cells expressing CA-WASp. (**A**) Timing from NEB to anaphase in U937 cells with and without CA-WASp expression, in the presence of DMSO or 20 μM CK666. (**B**) Timing from anaphase to the start of furrowing in U937 cells with and without CA-WASp expression, in the presence of DMSO or 20 μM CK666. (**C**) Timing from anaphase to the start of furrowing in HT1080 cells with and without CA-WASp expression, in the presence of DMSO, 20 and 40 μM M CK666. (**D**) Timing the duration of furrow closure in U937 cells with and without CA-WASp expression, in the presence of DMSO or 20 μM CK666. (**E**) Timing the duration of furrow closure in HT1080 cells with and without CA-WASp expression, in the presence of DMSO, 20 and 40 μM CK666. (**F**) Kymograph of a kinetochore pair showing oscillation imaged every 7.5 seconds.

Figure S5 Aurora B activity and cell division defects in cells expressing CA-WASp

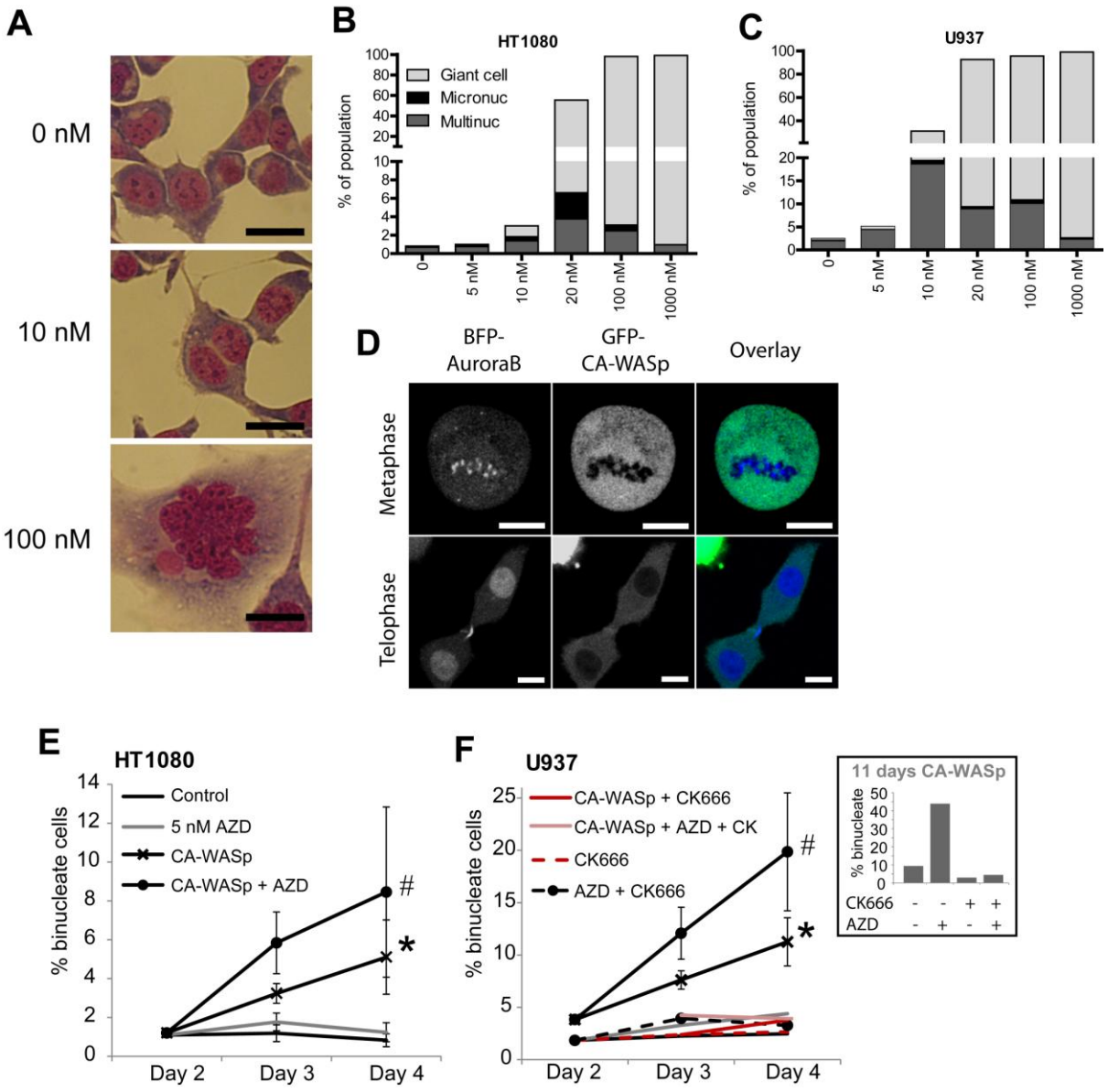

Figure S5. Aurora B activity and cell division defects in cells expressing CA-WASp. (**A**) Nuclear morphology showing binucleation and giant nucleus with increasing AZD concentrations. (**B,C**) AZD1152-HQPA was added to HT1080 (**B**) and U937 (**C**) cultures and mitotic slippage (giant cell), micronuclei formation and cytokinesis failure rates were measured. (**D**) Confocal microscopy of live HT1080 cells expressing Aurora B-BFP and GFP-CA-WASp. Bar = 10 μm. (**E**,**F**) HT1080 and U937 cells were transduced with GFP-CA-WASp, 48 hours later AZD1152-HQPA was added at 5 nM. The proportion of binucleated cells after 2, 3 and 4 days expression of CA-WASp is shown (n>3). (**F**) U937 cells were additionally treated with Arp2/3 inhibitor 1 day after transduction with GFP-CA-WASp. Inset shows the proportion of binucleated U937 cells after 11 days GFP-CA-WASp expression. * significant difference ($p<0.01$) from control, # significant difference ($p<0.01$) from CA-WASp.